

The problem of vaporizing flow of liquefied natural gas through porous flat joints of an LNG cargo containment system

Leelee Princess Lucky¹ and Emeka J. Okafor¹

¹Department of Petroleum and Gas Engineering, University of Port Harcourt

ABSTRACT: Liquefied natural gas (LNG) leakage into insulation walls of a Mark III type LNG cargo containment system (CCS) at above-boiling temperatures gives rise to complex fluid flow, heat transfer, and phase change processes. An example is LNG leakage into flat joints of an LNG CCS. The last decade has seen a strong increase of research into flows into insulation walls of CCS within LNG ships. Due to the flow characteristics, they challenge standard macroscale mathematical and numerical modeling of vaporizing flows. Thus, over the last decade, various modeling approaches have been developed to investigate this problem. This paper reviews common conceptual models and discretization approaches for vaporizing LNG flow through porous media, with an emphasis on the dominating effects the porous regions have on flow processes. In this context, the paper also discusses the tight connection between physical and mathematical modeling and simulation approaches, and points out potential extensions and/or research challenges related to transport, multi-phase flow with phase change and fluid-solid interaction. Examining a particular problem – the event of leakage through the primary barrier of an LNG CCS and a potential seepage through the flat joint. This raises the potential for cryogenic damage of the CCS and cargo tank failure as a result of the brittle fracture of the inner steel hull of the LNG ship.

KEYWORDS LNG; liquefied natural gas; vaporizing flow; heat transfer with phase change; porous media; LNG Cargo Containment System.

Date of Submission: 17-01-2023

Date of acceptance: 02-02-2023

I. INTRODUCTION

Natural gas has emerged the fastest growing energy resource in the world today due to the growing demand for low greenhouse gas emissions and high conversion efficiency in power generation [11]. Despite the drop in the global demand of natural gas by 1.9% or 75bcm (billion cubic meters) during the COVID-19 pandemic in 2020, research has proven that the global demand of natural gas rebounded by 3.6% in 2021 and unless there are major policy changes to curb global gas consumption, the demand will keep growing in the coming years even though it may happen at a slower pace but it is expected to reach nearly 4,300 bcm by 2024. This is a 7% rise from COVID-19 levels [22].

For domestic and intercontinental natural gas trade, LNG technology has proven to be the most viable means of transporting natural gas over long distances, from remote reserves around the world as shown in Figure 1 [15]. During transportation of natural gas via LNG Technology, the Cargo Containment System usually encounters damages, including sloshing damage, which results to leakage of LNG. Depending on the amount of leaked LNG permeating through the barriers of the insulation (see Figure 2), the inner hull steel structure may be exposed to the extreme low temperature of the cryogen resulting in potential yielding of the tank to brittle fracture.

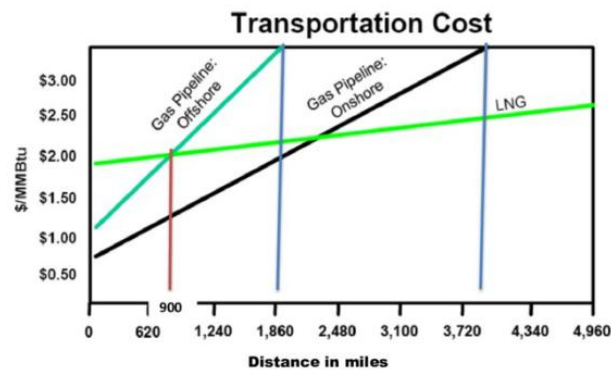


Fig.1.Comparison of gas transportation cost via gas pipeline and LNG[15]

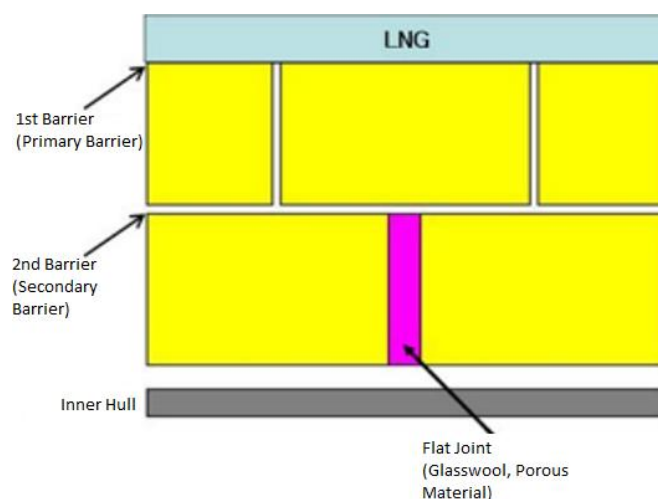


Fig.2.LNG CCS Insulation wall [6]

OVERVIEW OF LNG CARGO CONTAINMENT SYSTEM(CCS)

LNG is natural gas in liquid form obtained through the process of refrigeration. Natural gas is refrigerated to -260°F (-162°C) which permits long-term storage in tanks (rather than in underground reservoirs) and transportation by marine, road, or rail vehicle (rather than by pipeline). This very important resource is easily transported by ships when the consumers are located in coastal areas and by rail trailers or trucks when they are located on land. The ships are specialized LNG carriers which can consist of insulated double-hulled tanks, designed to contain the cargo slightly above atmospheric pressure at a cryogenic temperature of approximately -162°C . The LNG cargo containment system is the total arrangement within the ships for containing the cargo which includes:

- A primary barrier (the cargo tank)
- Secondary barrier
- Associated thermal insulation
- Any intervening spaces
- Adjacent structure, if necessary for the support of these elements.

LNG ships or carriers are largely classified as either Moss-type or membrane-type ships, and the CCS for membrane type ships are mainly divided into NO 96 or Mark III systems (see Fig. 3a and 3b) designed by Gaz Transport and Technigaz (GTT), France.

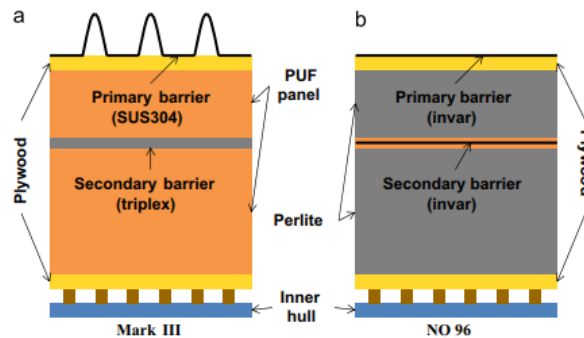


Fig.3.Schematic of insulation wall of a membrane-tank LNG Cargo Containment System [12]

The Gaz Transport membrane containment system (GT NO96) consists of a grillage structure made of plywood and filled with perlite in order to maintain tightness and insulation and the Technigaz membrane system (TG MARK III) consists of two layers of reinforced polyurethane foam separated by a material called triplex in order to configure an insulation system. However, latest containment system incorporates features from the existing GT No 96 and TG Mark III systems and uses reinforced polyurethane foam insulation and two membranes, the first one 0.7 mm thick made of Invar, the second made of a composite aluminum-glass fiber called triplex [12].

THE PROBLEM OF BARRIER LEAKAGE OF LNG CCS

During transportation of liquefied natural gas, the cargo containment systems of the LNG carrier usually encounter damages caused by sloshing impact loads. Damage to cargo containment system will result to leakage of LNG and of the two LNG carriers designed by Gaz Transport and Technigaz, Mark III system suffers a more serious issue when compared to the NO 96 system. This is because, the NO 96 system consists of plywood boxes with good mechanical properties, quite unlike the insulation barrier of the Mark III system that is made of polyurethane foam and glass wool. The Mark III is more vulnerable when subjected to internal and external shocks, with increased likelihood of LNG leakage. As illustrated in fig.2, the primary membrane (first barrier) contains the LNG cargo, while the secondary membrane (second barrier) which is identical to the primary membrane ensures a redundancy in case of leakage. In reality, the steel membrane could suffer from local cracks and the cryogenic fluid could flow through the primary insulation layer between the primary and secondary barriers. Further permeation through the secondary barrier will result to leaked cryogenic fluid flowing down the secondary insulation layer and depending on the amount, the inner hull steel structure may be exposed to the extremely low temperature and may eventually yield to brittle fracture [12].

II. PREVIOUS WORK ON VAPORIZING FLOW OF LNG THROUGH POROUS MEDIA.

Porous media flow with phase change provides particular challenges to modeling and simulation. These can be explained by the interaction between structural properties of the insulation wall with dynamic processes that takes place in the domain. The barriers and foams do, for example, strongly affect the nature of fluid velocities and penetration rates. Leading processes may not be well described due to introduction of strong discontinuities that are not well represented by averaged descriptions. Moreover, flow processes can also affect the nature of the liquid penetration fronts, for example due to mechanical or chemical fluid–solid interactions. In this section, the previous work for modeling vaporizing LNG flow through porous media is discussed, considering an insulation wall, particularly the flat joint. Let us now briefly review some of the works.

Bae *et al* (2003) [2] were among the first to conduct a failure mode and effect analysis (FMEA) of a Mark III type CCS where they also used a simple fluid dynamic model to estimate the correlation between leakages in the secondary barrier and its effect on the cargo containment system's capacity to safely contain the cargo. The LNG leak phenomena was simulated using a commercial computational fluid dynamics (CFD) tool with the boundary conditions as shown in Fig.4. They selected the most severe leak condition - leak position at bottom primary barrier, with secondary leak position just below the leak position at primary barrier. They assumed that a primary barrier leakage hole is open enough to allow LNG flow into secondary barrier leaked area. However, their work did not elucidate the complex vaporizing flow of the leaked LNG down the flat joint, an important problem that could give important insights on liquid penetration rates and the potential duration of seepage onto inner hull of the LNG CCS.

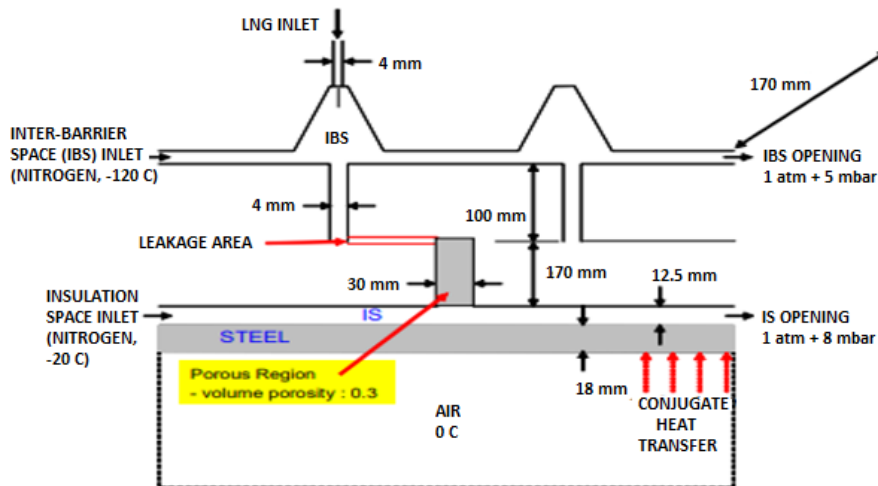


Fig.4. Boundary Condition for CFD Analysis [2]

Park *etal*(2009)[6] experimentally investigated the behavior of leaked LNG flow in the secondary insulation layer of a cargo containment system and experimental conditions were simulated using computational fluid dynamics (CFD) code. The experimental and computational results suggest that, unless there is a massive leak, the cryogenic fluid mostly evaporates in the insulation system and does not reach the inner hull (see Fig.2) in the liquid state. Although a single fluid mixture multi-phase flow model was used to handle the vaporization of the LNG, important details regarding the liquid penetration depth and duration of seepage through the flat joint were not provided.

Lee *etal*(2012)[9] conducted a thermal analysis of a CCS insulation box to determine the temperature distribution of the CCS insulation box using experimental database and also developed a computational method for the prediction of the temperature in an insulation wall system with leaking LNG. Results reveal that the leaked LNG vaporized as it flows downwards through the porous region (flat joint) since the temperature in the insulation layer of the cargo tank was maintained at the normal temperature. Also, the rapid temperature drop as displayed in Fig.5 with increasing leakage hole (inlet) sizes suggest that the allowable crack size can be estimated by their computational method but this should be limited to less than 5mm. However, seepage duration and depth of penetration through the porous region were not modeled.

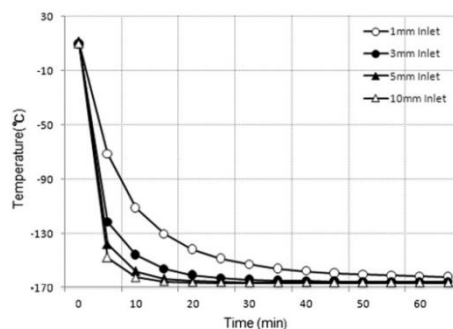


Fig.5. Time History of Temperature For various inlet sizes; No 13 Thermocouple [9]

Choi *etal* (2012)[10] experimentally determined the thermal conductivity of the insulation materials used in cargo containment system following seepage through insulation walls of the CCS. Results as shown in Fig. 6 reveal that thermal conductivity decreases as the environmental temperature decreases. Also, results show that some amount of leaked LNG can be evaporated and possibly move out of the cargo containment system due to great temperature difference between the LNG and the environment. However, the heat flow in porous media while considering the phenomenon of vaporization by means of multi-phase effect calculations of liquid and LNG gas was not considered. We need such information to properly characterize the influence of multi-dimensional heat transfer on vaporization rate.

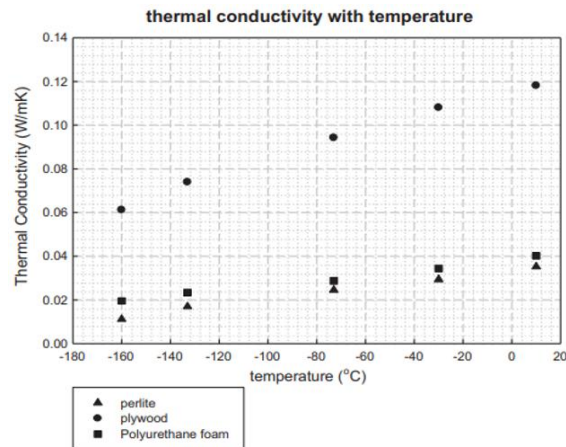


Fig. 6. Temperature-dependent thermal conductivity for Perlite, Plywood and Polyurethane foam[10].

Lee *et al*(2015)[12] investigated the diffusion speed and the vapor/liquid composition changes of the leaked LNG through the modified NO96 (NO96 GW) insulation box shown in Fig. 7. The primary and secondary barriers of NO 96 system are made of thin sheet of mickey alloy called invar and the insulation system comprises of two layers of plywood boxes filled with perlite as shown earlier in Fig.3.The primary insulation box shown in fig. 8

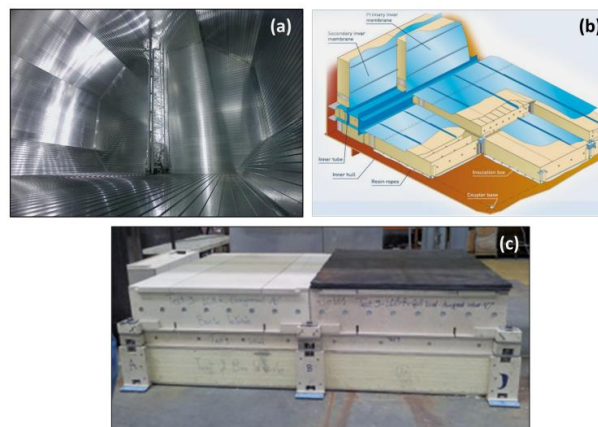


Figure 7: (a) Inside view of NO96, (b) the configuration of flat NO96 insulation and (c) the modified NO96 insulation system (GTT).[12]

is composed of plywood box filled with glass wool. Once the insulation boxes are filled with leaked LNG, heat transfer rate from outside to the cargo is greatly changed resulting in significant degradation of the insulation performance which in turn leads to great loss of LNG. A CFD (computational fluid dynamics) model was used to simulate the diffusion behavior and the heat transfer characteristics of leaked LNG including the liquid-to-gas phase change through porous structure. The CFD model considered phase change, gas-liquid reactions in the porous media and the accompanied rates of heat transfer. It also considered the geometry of NO96 membrane storage facilities with glass wool and plywood. In the numerical simulation, the LNG pool spreading, heat diffusion, and the evaporation were investigated. An inlet pressure of 1atm, and for comparison, 0.5 atm corresponding to filling ratio of 50%, on the crack location of 15m (h), as shown in figure 9, were employed for the analysis. In their numerical simulation, the LNG pool spreading, heat diffusion, and the evaporation were investigated. Numerical result reveals that the diffusion speed through the insulation box was very fast and the glass wool was not suitable to satisfactorily delay the leaked flow. Also, the effect of porosity on the leaked flow diffusion was not investigated.

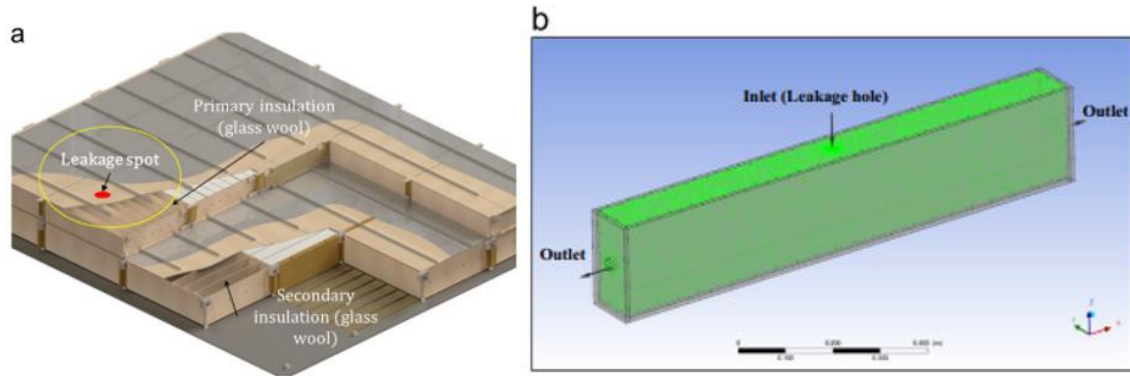


Fig.8.Schematic of modified NO96 (a) CCS insulation system and (b) primary insulation box[12].

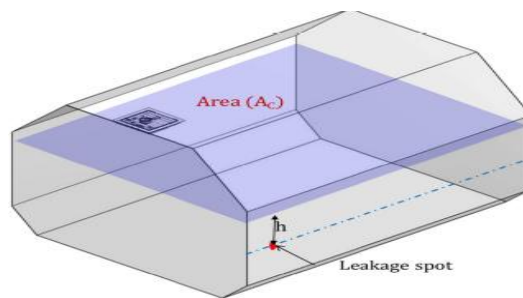


Fig. 9. LNG CCS with Leakage spot[12]

Choi *et al*(2015)[13] performed an experimental investigation of the behavior of cryogenic liquid in porous media with various densities using a square section cylinder (SSC) and a rectangular duct(RD).LNG leakage is more likely to occur in the foam layer type markIII system where the insulation barrier is made of polyurethane foam and glass wool (see figure 10).To simulate the LNG leakage, a cryogenic liquid was injected into moulds with glass wool samples of three different bulk densities with diameters of about 14.Μm and spherical balls were used as the porous medium as shown in figs. 11 and 12.To obtain the permeability

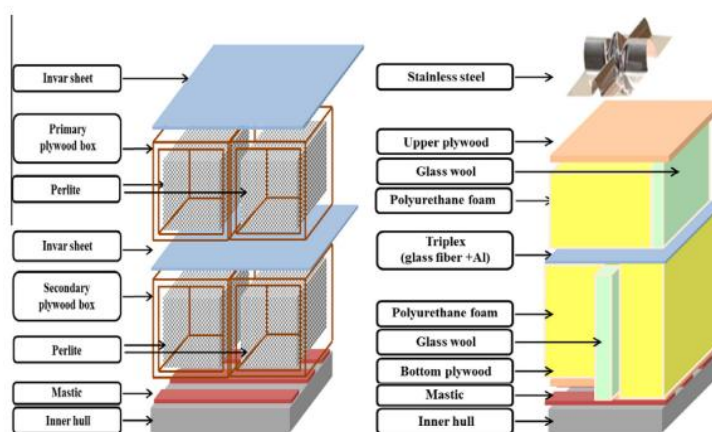


Fig. 10.LNG cargo containment system and each composition (left; NO 96 system, right; Mark III system)[13].

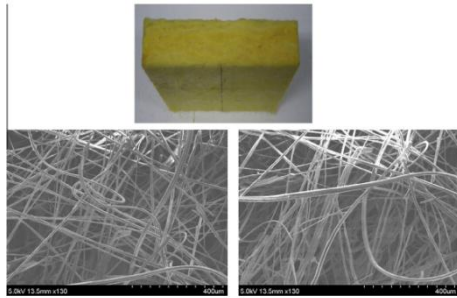


Fig. 11.Features of glass wool[13].

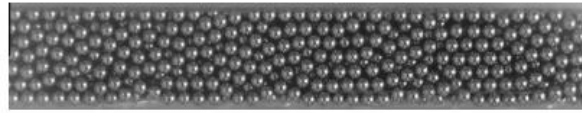


Fig.12. Spherical steel balls for exp. experiment [13].

of the glass wool used for their study, an experimental apparatus (see fig. 13) was set up; glass wool samples of different dimensions were placed on the lower mold and silicone oil was injected into the cavity using a fluid injection pump while the pressure was continuously recorded using pressure transducers. In the two distinct experiments with their respective experimental setup (not shown); temperature and pressure were measured to determine the phase state of the flow in glass wool media with different bulk densities. In summary, experimental results from Choi and co-workers reveal that the pressure drop was greatly influenced by the phase transition, and the liquid-phase saturated area depended on the phase state, which was determined by the temperature and pressure and the time taken for saturation in this area increased with increasing bulk density. Numerical simulation conducted was in good agreement with experimental results but modeling of seepage depth and duration were not detailed.

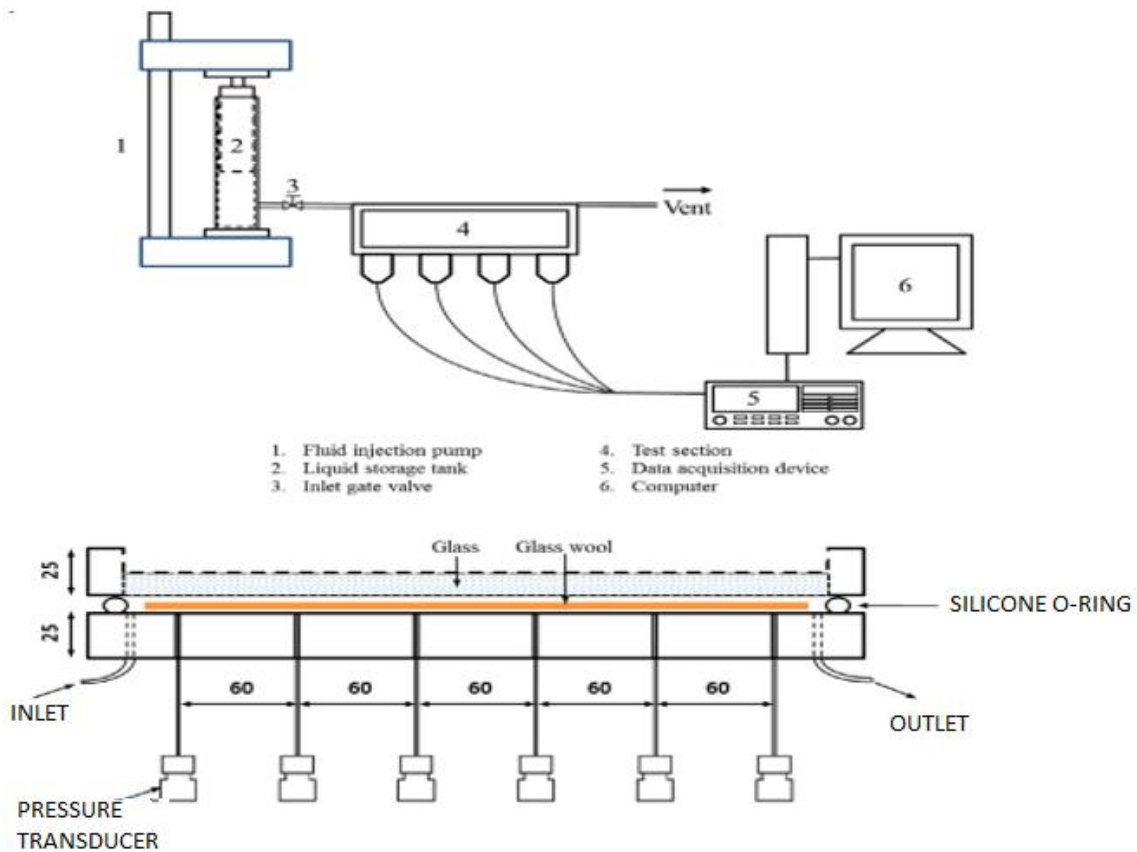


Fig. 13.The schematic illustration of the permeability measurement apparatus and its test section (all dimensions are in mm)[13]

Chan (2015)[14] numerically and experimentally studied the evaporation of a cryogen in an insulating porous medium. The flow and heat transfer characteristics around the evaporating cryogenic gas in the medium was analyzed based on the VOF (Volume of Fluid) method. The thermal leakage through the porous medium to the outer shell was also analyzed using heat transfer considerations. To support the numerical results, an

experiment, illustrated in fig. 14 was performed using LNG as the fluid and glass wool as the porous medium. The numerical results for the outer shell temperature predict the experimental values well. Based on the validated numerical results, the transient behavior of temperature distribution in outer shell was analyzed. The effect of crack size on the reliability of insulation system was investigated. The behavior of the virtual evaporation velocity and the liquid film area was considered qualitatively. Although, this work sheds light on technology related to cryogenic storage systems by suggesting a systematic method for predicting the temperature of the outer shell, the liquid film area, and virtual evaporation velocity, more work regarding the depth of penetration in the porous medium is required.

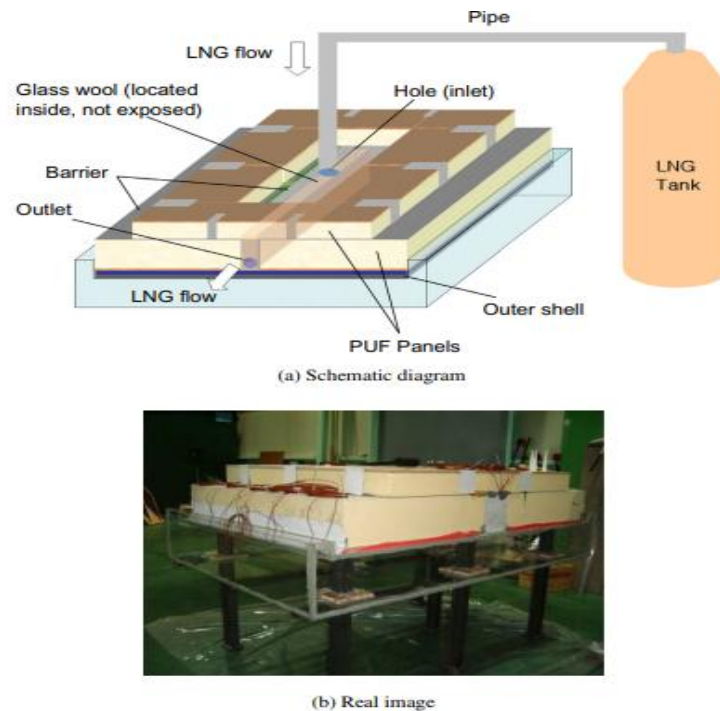


Fig. 14. Chan's Experimental Apparatus [14]

Choi *et al* (2016) [16] did further work on this problem where they conducted a conjugate heat transfer analysis of LNG leakage in CCS to investigate the phase change and heat transfer behaviour when a liquefied natural gas (LNG) leakage occurs. The Mark III CCS consists of two separate spaces that are filled with insulation materials to keep higher thermal efficiency as shown in fig. 15. The behavior of cryogenic liquid in a porous structure and the resulting temperature change of the hull's plate was estimated using numerical simulation and according to the numerical study, the thermal safety of the hull's plate is guaranteed in a case where the LNG leakage hole is 2mm in diameter. Although, the amount of time leakage was retained in the flat joint and the temperature distribution of the hull's plate for the leaked LNG was identified, porosity and permeability modelling and their effects on penetration rates were not adequately investigated.

Mario *et al* 2016 [17] investigated the heat transfer from the external environment to the liquefied natural gas (LNG) stored inside a 165,000 m³ capacity ship carrier containing 4 mark III tanks following the arrangement and prismatic shapes shown in fig. 16 and having the characteristics dimensions (not shown). The assembly of the flat panels and corners shown in figure 17. Four successive approaches illustrated in fig. 18 were developed to obtain the heat flow transferred from the environment to the LNG, based on simplified numerical simulations and reduced order models of heat transfer through the insulation barriers of LNG tanks. Although results obtained were in line with published data, experimental boil off rate (BOR) data during real ship transportation that would have provided useful information to validate the numerical approaches used was not available.

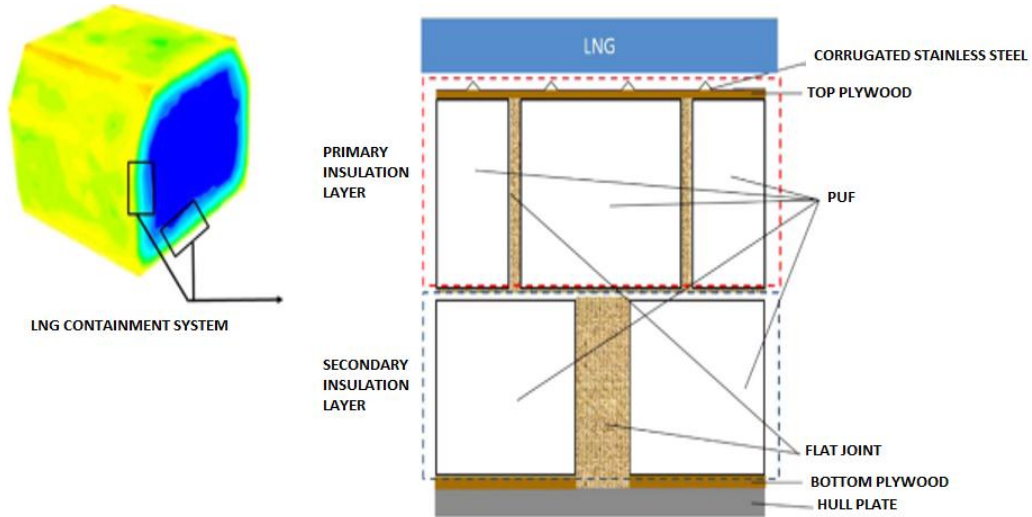


Fig.15. The assembly description of the Mark III system[16].

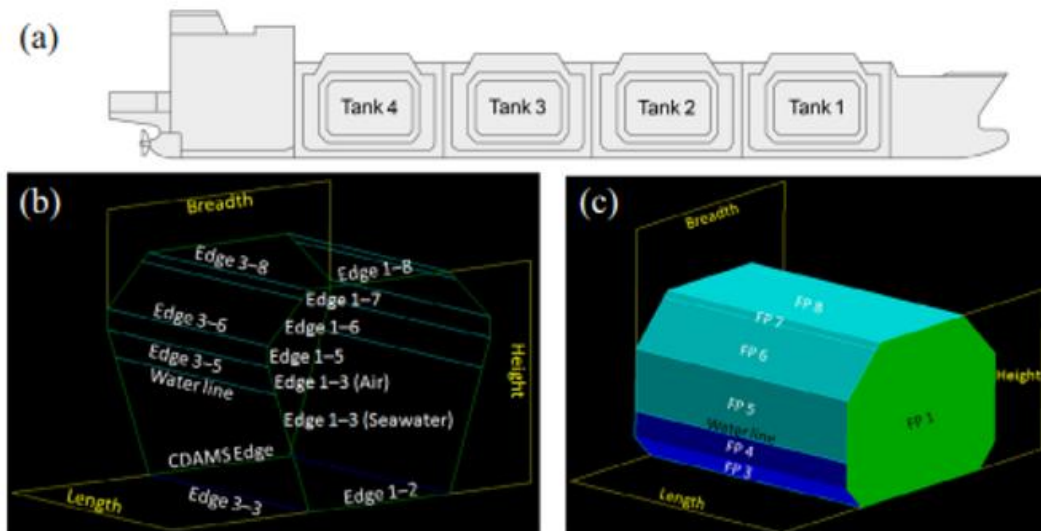


Fig.16.(a) Tank layout; (b) Tank 1: dimensions and names of edges; (c) Tanks 2, 3 and 4: dimensions and names of Flat Panels (Flat Panel 2 is the base of the tank)[17].

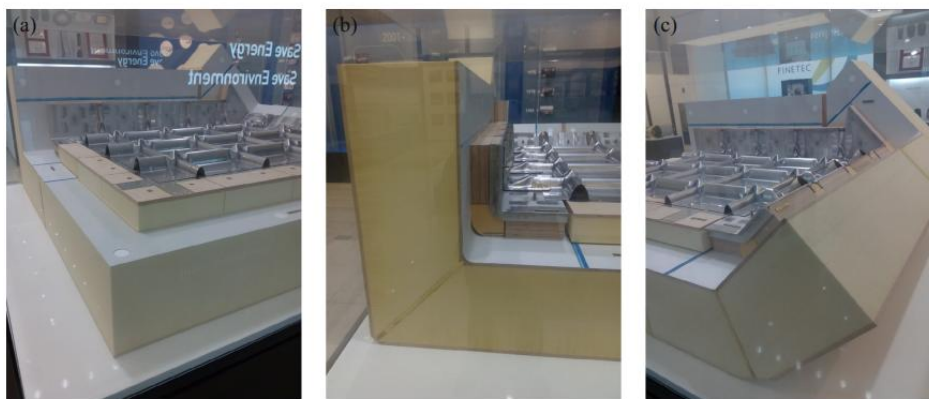


Fig.17. Insulation barriers: (a) Flat Panels; (b) 90° Corner; (c) 135° Corner and Trihedron[17].

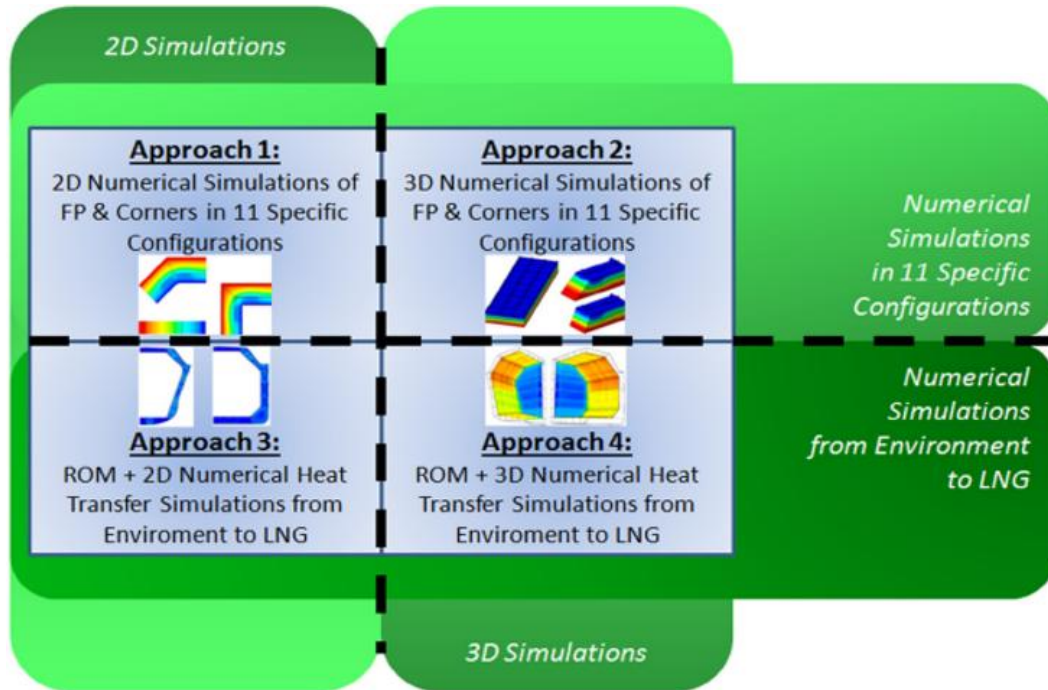


Fig.18.Approaches for BOR calculation [17]

Niu et al (2017)[18] proposed a new independent type B CCS to meet the targets of cryogenic reliability and high thermal insulation performances. The primary barrier of Mark III system is made of corrugated stainless steel and directly supported and fixed to the insulation panels while the primary and secondary barrier of NO 96 system are made of invar. The new independent type B LNG is a prismatic tank and they presented a comparative study of these two designs. Figs. 19 and 20 show a thermal insulating system they developed with installation and cost advantages. They argue that the new design can efficiently prevent environment heat inflow for the LNG vaporization and ensure the safety for the inner hull structures of the LNG Carrier. However, the vaporizing flow studies were not adequately delineated.

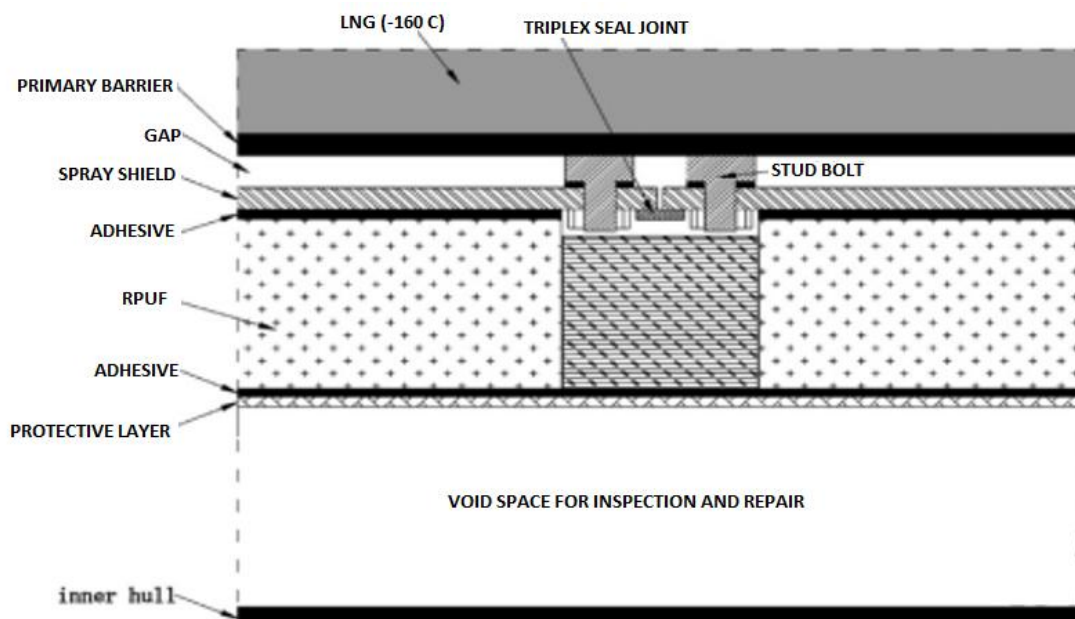


Fig.19.Schematic diagram of the thermal insulation system for the new independent type B CCS[18]

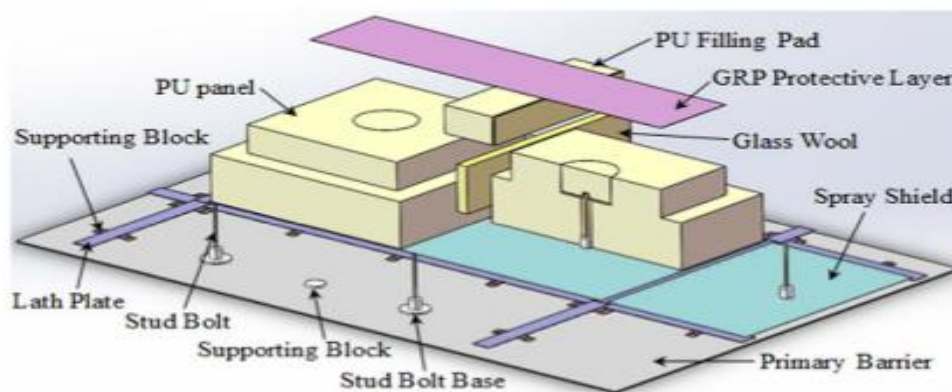


Fig.20.Schematic of the thermal insulation system of new independent type B LNG Carrier[18].

Yongfeng et al (2019)[21]described the numerical method implemented in Gas Transport and Technigaz specific purpose thermal and thermodynamic code for complex physical phenomena in liquefied natural gas (LNG) carrier tanks (see Fig. 21).Validations of the full thermal-thermodynamic model were performed through a comparison with onboard observation datasets. The model successfully simulated the liquid and gas temperature evolution and the variation of pressure within the ballast and laden voyages for a period up to 3 days. As a demonstration of the ability of the model, the operational Boil-Off was investigated by integrating the actual sailing conditions, the thermal inertia of the CCS, sea conditions and unsteady evolution of LNG and NG. During a laden voyage profile of a case study LNG carrier, they evaluated their model with onboard experiment including the comparison with the measured natural BOG, forced BOG data, etc.The results show the importance of taking into account operating profile in pressure and in engine consumption to represent the variability of the BOG under real onboard conditions.The rigorous modeling of the LNG evaporation phenomenon can make a significant contribution to industry and science. However, the heat conduction aspects were not fully investigated.

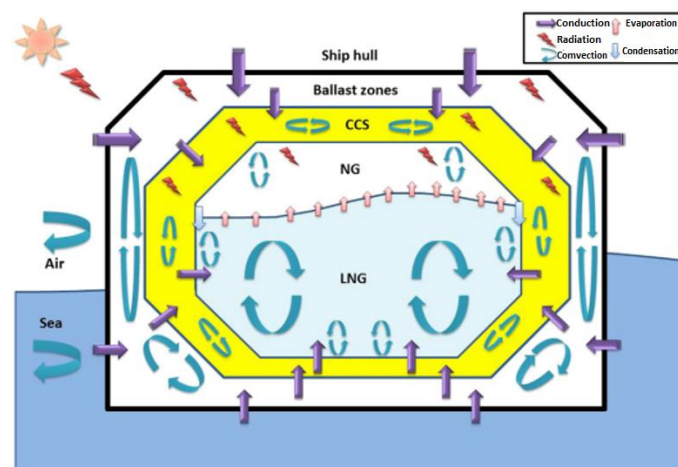


Fig. 21.Schematic representation of the different physical phenomena in the Tank [21]

III. POROUS MEDIA PERMEABILITY ESTIMATION FOR VAPORIZING FLUID FLOW

Permeability has long been introduced into Darcy's equation where it is used to characterize porous media and its associated flow (see equation (1) below). Permeability estimation is of crucial importance for the description of different physical processes such as fluid circulation in geothermal systems, fluid flow in oil and gas reservoirs, and fluid flow through various porous substrates encountered in nature. The formulation of satisfactory theoretical model for permeability of porous media has been difficult mainly due to the complexity of the substrate geometry and the intricate nature of connected pore spaces [19].

Three (3) methods are commonly used for permeability estimation:

- 1) Conventional well testing or field pumping or injection testing that gives a reliable estimation of the field permeability. This method is however expensive and time consuming.

- 2) Measurement of pressure drop, and gas or liquid flow through samples in laboratory experiments. This method is designed for consolidated media.
- 3) Use of empirical relationships between permeability and porous medium textural parameters such as porosity, surface to volume ratio, tortuosity of the void space, pore connectivity, grain and pore shape, and size distribution of the sample.

Permeability estimation based on the Kozeny-Carman equation (see equation (2)) is widely accepted and used in the field of flow in porous media. However, a short coming of the Kozeny-Carman equation is that it does not account for the effects of diagenetic changes in pore radius for grain size permeability estimation. Also, it is impractical to measure tortuosity, shape factor and specific surface area for different porous media. In other words, conventional Kozeny-Carman equation does not characterize the microstructure of a porous medium. However, the classical Kozeny-Carman equation can be an acceptable approximation, as demonstrated in the work of Okafor (2013) where he estimated permeability of a fibrous porous media being penetrated by LNG.

However, the Kozeny-Carman equation still requires improvement as attested to from the work of Rodriguez et al (2004) [3] who investigated permeability-porosity relationship for glass and natural fibers. Their results show that the Kozeny-Carman equation cannot fit all the data well unless both parameters C and n (see equation (3)) are changed for different fiber mats.

$$v = - \left(\frac{K}{\mu} \right) \nabla p \quad (1)$$

$$K = \frac{1}{C_{KC}} \cdot \frac{\phi^3}{S^2 \tau^2} \quad (2)$$

$$K = c \frac{\phi^{(n+1)}}{(1-\phi)^n} \quad (3)$$

In equations (1), (2) and (3), K denotes permeability, τ is Tortuosity, ϕ is porosity, C_{KC} is Kozeny-Carman constant, and S is the specific surface area. The c and n are empirical parameters.

Xu and Yu 2008 [5] derived a model (Equation 4) based on the fractal dimensions, porosity and the pore size after a thorough review of the Kozeny-Carman equation. They added a constant coefficient which was obtained from the assumption of a square geometry model. Their model is closely related to the microstructures in porous media and as such will provide a better understanding of flow and permeability in porous media.

$$K = \frac{1}{36 C_f} \frac{\phi^{(3-D_T)/2}}{(1-\phi)^{(1-D_T)/2}} \quad (4)$$

The coefficient C_f in equation (4) is $= \frac{\pi D_f^{(1-D_T)/2} [4 + (2-D_f)] 1^{(1+D_T)/2}}{128(3+D_T-D_f)}$

D_f and D_T are fractal dimensions and tortuosity fractal dimension, respectively. Costa (2004) [4] reviewed Kozeny-Carman model using the hypothesis of a fractal pore-space geometry and empirically based Archie law. He formulated his model without introducing the concept of hydraulic radius and obtained a new simple permeability equation which successfully predicted permeability of different non-granular systems such as fiber mats and vesicular rocks.

$$K = C_c \frac{\phi^m}{(1-\phi)} \quad (5)$$

C_c in equation (5) is a factor like the Kozeny coefficient and m is the Archie exponent. Civan (2002) [1] addressed the assumption in Kozeny-Carman equation of flow within impermeable pores by representing tortuous natural flow path as leaking capillary tubes. He then introduced a pore connectivity parameter, as shown in equation (6), of unknown physical significance that governs flow between tubes. His model is not verified when compared with observational data.

$$\sqrt{\frac{K}{\phi}} = \alpha \left(\frac{\phi}{\alpha - \phi} \right)^2 \quad (6)$$

Henderson et al (2010)[7] deduced a three parameter Kozeny-Carman equation using fractal theory and obtained numerical results by fitting experimental data which revealed that their generalized equation (see equation (7)) can describe the permeability-porosity relationship of many natural and industrial materials such as sandstone, sisal fiber mats and glass fiber fabrics. This is expressed as,

$$\sqrt{\frac{K}{\phi}} = \xi \frac{\phi^{(\xi+2)/2}}{(1-\phi)^{1n}} \quad (7)$$

where $\xi = D_{\tau} \geq 0$, $n = D_{1/m} b > 0$

$$\xi = (C_{\square}^{1/2} C_{1/m_g/f}) \geq 0$$

D_{\square} = Fractal exponent of \square

C_{\square} = Fractal coefficient of \square

Yazdchi et al (2011)[8] modified Kozeny-Carman equation for flow paths in the narrow pore throats of rocks for a wide range of porosities (equation 8). Their equation is based on series of finite element modelling obtained from unidirectional random arrays of fiber cylinders which cannot represent real porous media.

$$\frac{K}{d^2} = \frac{\xi^3}{\psi \left(\frac{L_e}{L}\right)^2 (1-\xi)^2} \quad (8)$$

Nomura et al (2018)[20] presented a modified model of the Kozeny-Carman equation based on a sigmoid function. Their study demonstrated that the specific surface area can be derived from the semilog sigmoid functions which simplify but accurately represent the soil particle size distribution but the error of their model (see equation 9) exceeded 20.1%.

$$K = \frac{1}{36\pi^2 k_o} \frac{\rho_w g}{\mu} \left[D_{50} \frac{\ln 13.50}{\ln C_u} \sin \left(\frac{\pi \ln C_u}{\ln 13.50} \right) \right]^2 \frac{\psi^3}{1+\psi} \quad (9)$$

IV. CONCLUSION

This paper has reviewed mathematical models, physical models and numerical approaches developed to model vaporizing fluid flow in porous media, particularly those found within insulation layers of large LNG cargo containment systems. This has been an interesting research field and new modelling concepts and discretization techniques to handle a range of situations relating to vaporizing flow within insulation layers, where heat transfer and vaporization rate, dominate are still needed to address the substantial challenges encountered in dealing with such multi-phase flow and multi-physics couplings within such geometry. To investigate the flow behaviour in porous media, the material properties of the porous structure must first be determined and permeability: a key parameter for analysing flow behaviour must be determined correctly. We also reviewed some of the merits and demerits of the Kozeny-Carman equation. A correctly estimated permeability model based on any of the available correlations or improved versions of the permeability relationship can be coupled to the vaporizing flow model with predictions generic enough to describe vaporizing fluid flow (including LNG flow) down porous regions of an insulation layer housing the flat joint of a Mark III cargo containment system. The new models that address the salient gaps should be extensively validated to increase the certainty of model predictions.

REFERENCES

- [1]. Civan, F., Yazdchi, k., Srivastava, S. and Luding, S.: On the validity of the Carman – Kozeny equation in random fibrous media. II International conference on particle –based methods – Fundamentals and applications (2011).
- [2]. Bae, J., Joh, k., Yoon, H., Lee, H. and Ha, M.: Safety Evaluation of Mark III Type LNG Carriers under Barrier Leakages (2003).
- [3]. Rodriguez, E., Giacomelli, F. and Vazquez, A.: Permeability – Porosity Relationship (2004).
- [4]. Costa, A.: Permeability- porosity relationship: A reexamination of the Kozeny –Carman equation based on a fractal pore-space geometry assumption. Geophysical Research Letters. Vol. 33(2006).
- [5]. Xu, P. and Yu, B.: Developing a new form of permeability and Kozeny – Carman constant for homogeneous porous media by means of fractal geometry, Advances in Water Resources 31: 74 -81(2007).
- [6]. Park, J.B., Lee, B.H., Rhee, S.H., Bae, J.H., Lee, W.K., Jeong, J.W. and An, J.S.: Cryogenic fluid flow in the insulation wall of the cargo containment system. Retrieved 28/11/2021 <http://proceedings.asmedigitalcollection.asme.org> (2009).
- [7]. Henderson, N., Juan, C.B., Wagner, F.S.: A three – parameter Kozeny – Carman generalized equation for fractal porous – media. Chemical Engineering Science, 65: 4432 – 4442(2010).
- [8]. Yazdchi, k., Srivastava, S. and Luding, S.: On the validity of the Carman – Kozeny equation in random fibrous media. II International conference on particle –based methods – Fundamentals and applications (2011).

- [9]. Lee, B.H., Park, B.J., Rhee, S.H., Bae, J.H., Lee, W.K. and Jeong, J.W.: Liquefied natural gas flow in the insulation wall of a cargo containment system and its evaporation. *Applied Thermal Engineering*, 31: 2605 -2615(2012).
- [10]. Choi, S.W., Kim, S.H. and Lee, W.I.: Analysis of two main LNG CCS (Cargo Containment System) insulation boxes for leakage safety using experimentally defined thermal properties. *Applied Ocean Research*, 37: 72 – 89(2012).
- [11]. Mokhatab, S., John, Y., Jaleel, V., Valappil, S., David, A.W.: *Handbook of Liquefied natural gas*, first edition. Gulf professional publishing, Burlington, MA, USA (2014).
- [12]. Lee, J.H., Kim, Y.J., and Hwang, S.: Computational study of LNG evaporation and heat diffusion through a LNG cargo tank membrane. *Ocean Engineering*, 106:77-86(2015).
- [13]. Choi, S.W., Lee, W.I. and Kim, S.H.: Analysis of flow characteristics of cryogenic liquid in porous media. *International journal of heat and mass transfer*, 87:161-183(2015).
- [14]. Chan, B.: Numerical study on the phase change heat transfer of LNG in glass wool based on VOF method. *International journal of heat and mass transfer*, 88: 20 – 27(2015).
- [15]. Ahmed, A.: Using natural gas to meet Latent energy demand in Nigeria and economic advantage. DOI: 10.13140/RG.2.2.26908.95368 (2016).
- [16]. Choi, S.W., Kim, S.H. and Lee, W.I.: Analysis of leaked LNG flow and consequent thermal effect for safety in LNG cargo containment system. *Ocean Engineering*, 113:276-294(2016).
- [17]. Mario, M.A., Regina L., David, D. and Young, H.H.: Calculation of Boil-Off Rate of Liquefied Natural Gas in Mark III tanks of ship carriers by numerical analysis. *Applied Thermal Engineering* 93: 279–296(2016).
- [18]. Niu, W.C., Lia, G. L., Jua, Y.L. and Fu, Y.Z.: Design and analysis of the thermal insulation system for a new independent type B LNG Carrier. *Ocean Engineering* 142: 51 – 61(2017).
- [19]. Taheri, S., Ghomeshi, S. and Kantzas, A.: Permeability calculations in unconsolidated homogeneous sands. *Powder Technology* (2017).
- [20]. Nomura, S., Yamamoto, Y. and Sakaguchi, H.: Modified expression of Kozeny – Carman equation based on semi log – sigmoid function. *Soils and Foundations*, 58: 1350 -1357(2018).
- [21]. Youngfend, Q., Ibrahima, N., Xiaochun, X., Romain, P. and Jean N.J.: A thermal and thermodynamic code for the computation of Boil-Off Gas – Industrial applications of LNG carrier. *Cryogenics* 99: 105 – 113(2019).
- [22]. IEA: World Outlook 2021. International Energy Agency Publications. Retrieved 28/11/2021. www.iea.org/weo
- [23]. Okafor, E.: Modelling vaporizing fluid flow through porous media with applications to liquefied natural gas, Imperial College London PhD Thesis, (2013).